

# Where is also about time: A location-distortion model to improve reverse geocoding using behavior-driven temporal semantic signatures

Grant McKenzie, Krzysztof Janowicz

*The STKO Lab, Department of Geography, University of California, Santa Barbara, CA, USA*

---

## Abstract

While geocoding returns coordinates for a full or partial address, the converse process of reverse geocoding maps coordinates to a set of candidate place identifiers such as addresses or toponyms. For example, numerous Web APIs map geographic point coordinates, e.g., from a user's smartphone, to an ordered set of nearby Places Of Interest (POI). Typically, these services return the  $k$  nearest POI within a certain radius and measure distance to order the results. Reverse geocoding is a crucial task for many applications and research questions as it translates between spatial and platial views on geographic location. What makes this process difficult is the uncertainty of the queried location and of the point features used to represent places. Even if both could be determined with a high level of accuracy, it would still be unclear how to map a smartphone's GPS fix to one of many possible places in a multi-story building or a shopping mall. In this work, we break up the dependency on space alone by introducing time as a second variable for reverse geocoding. We mine the geosocial behavior of users of online location-based social networks to extract temporal semantic signatures. In analogy to the notion of scale distortion in cartography, we present a model that uses these signatures to distort the location of POI relative to the query location and time, thereby reordering the set of potentially matching places. We demonstrate the strengths of our method by evaluating it against a purely spatial baseline by determining the Mean Reciprocal Rank and the normalized Discounted Cumulative Gain. Our method performs substantially better than said baseline.

**Keywords:** Reverse Geocoding, Point of Interest, Semantic Signature, Geosocial Check-in, Time

---

## 1. Introduction and Motivation

Translating back and forth between spatial and placial representations of location is a crucial task underlying many research questions, applications, and systems. Geocoding, for instance, is the process of assigning corresponding geographic coordinates to other types of structured geographic identifiers such as addresses. The converse process, called reverse geocoding, assigns place identifiers, such as toponyms, to geographic coordinates. More specifically, it maps a geometry in the sense of OGC's Simple Feature model to an ordered set of candidate place identifiers. Typically, the Euclidean distance between the query coordinates and the point-feature representation of the candidate places is used to establish a relevance ranking. To successfully match a user's location to a visited place, new geosocial approaches also consider popularity, e.g., how many users checked-in or wrote reviews about a place. Additionally, many (reverse) geocoding systems consider place hierarchies and granularity.

The following queries nicely illustrate the difference between a spatial and placial perspective as well as the arbitrariness of relying on point coordinates for the query and the candidate places alone. While not a reverse geocoder in the strict sense, the Flickr `flickr.places.findByLatLon` API call [8] returns place IDs given a lat/lng coordinate and accuracy value. This allows users to find photos for particular places. The API *rounds up* to the nearest place type, i.e., it returns a city ID for street-level coordinates rather

---

*Email addresses:* grant.mckenzie@geog.ucsb.edu (Grant McKenzie), janowicz@ucsb.edu (Krzysztof Janowicz)

than returning a street or building. Latitudes and longitudes are truncate to three decimal points. In each case shown below, the query coordinates represent the same fix at the Griffith Observatory in Los Angeles. However, the query is run with different accuracy levels where 16 corresponds to the street level, 11 to the city level, and 7 to the county level. The respective responses from the Flickr API are as follows.<sup>1</sup>

```
<places latitude="34.118341" longitude="-118.300458" accuracy="16" total="1">
  <place place_id="HqDLYDJTUb8XihsYDg" woeid="23511984" latitude="34.125"
    longitude="-118.306" [...] place_type="neighbourhood" place_type_id="22"
    timezone="America/Los_Angeles" name="Hollywood United, Los Angeles, CA, US,
    United States" woe_name="Hollywood United" />
</places>
```

```
<places latitude="34.118341" longitude="-118.300458" accuracy="11" total="1">
  [...] latitude="34.146" longitude="-118.248" [...]
  place_type="locality" place_type_id="7" name="Glendale, California,
  United States" [...] /> [...]
```

```
<places latitude="34.118341" longitude="-118.300458" accuracy="6" total="1">
  [...] place_type="county" place_type_id="9" [...] name="Los Angeles County,
  California, United States" [...] /> [...]
```

The fact that even small differences in spatial accuracy may have strong impacts, e.g., on routing choices, has been demonstrated in the literature before [3]. What makes the example above interesting is the place hierarchy. Hollywood is a district of Los Angeles, while Glendale is a city in Los Angeles County. From a human-centered *placial* perspective, one would assume the queries to return Hollywood (in fact, it should be the Los Feliz neighborhood), Los Angeles, and finally Los Angeles County. Instead the neighboring city of Glendale is returned for the city-level accuracy query, thereby breaking the expected hierarchical composition of places. From a computation-centric *spatial* perspective Glendale is returned by the Flickr API simply because its centroid representation is closer to the query location than the centroid of Los Angeles.

The arbitrariness and imprecision of point-feature representations as well as the effect of missing topological relations also strikes on the level of small-scale features such as Places Of Interest (POI).<sup>2</sup> Figure 1 illustrates a common issue. First, the resort marker (A) is placed at the entrance to the parking lot. While this may be acceptable, other POI databases place it at the center of the building which is nearly 150m away. Second, the lounge is *inside* the resort but its marker (B) is shown over 100m away from the resorts marker. As most reverse geocoders rely on distance alone, such differences will lead to substantially different and often misleading results, e.g., when suggesting a user's check-in location.

As the omnipresence of location-enabled mobile devices increases, more robust, accurate, context-aware, and data-rich geolocation services are required. Today, the ability to link spatial coordinates to an actual place has become essential in many aspects of our everyday lives including navigation applications, place recommendation, location-based advertising, and critical infrastructure. It is interesting to note that the challenge is not one of more accurate GNSS and Wi-Fi-based positioning systems (WPS) alone. The information that a person checked-in or is present at a place is *semantically richer* than the spatial data alone. To give a concrete example, the fact that a person is standing in front of a *food truck* is substantially different from the fact that a person checked-in to the *food truck* and is likely to order something. Placial information is more than just spatial proximity.

Commercial companies such as *Google* as well as open source platforms like *GeoNames* have made names for themselves offering application programming interfaces (APIs) and web services that allow both developers and consumers to query gazetteers and POI databases using geographic coordinates as input. With the increase in user-generated geo-content, new services such as *Foursquare* and *Yelp* have emerged allowing anyone with a location-enabled mobile device to contribute or update the location of an entity in a crowd-sourced system. It is important to note that while these systems involve the contribution of geo-content from individual users, there is still some discussion as to whether or not they fit in to the category

---

<sup>1</sup>The remainder of the paper will use data from the location-based social network Foursquare.

<sup>2</sup>Frequently also referred to as *Points Of Interest*.

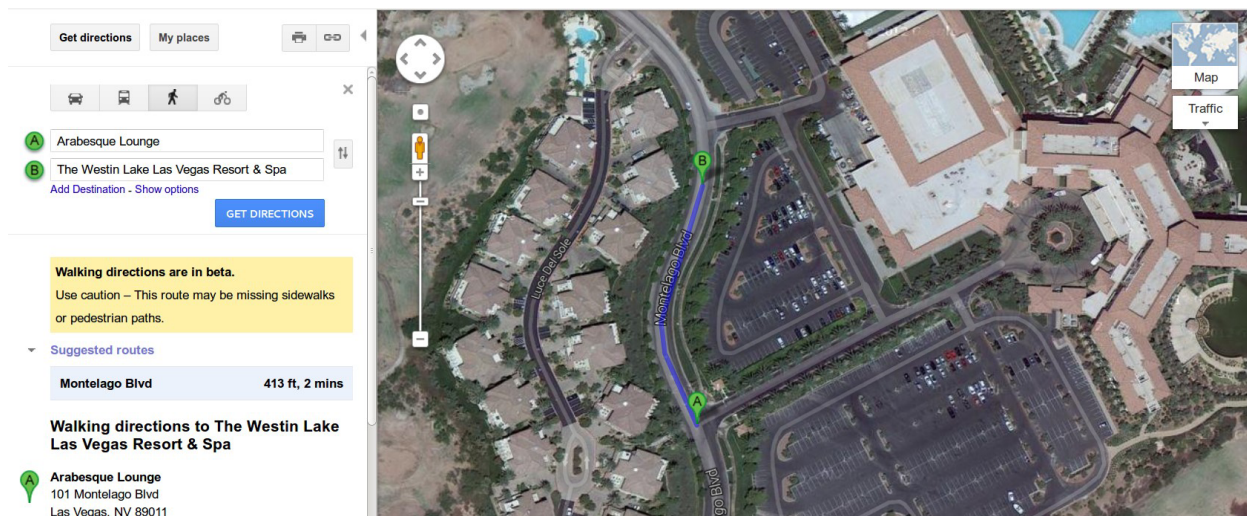


Figure 1: Point-feature distance between a resort and the lounge located inside of it (screenshot from Google Maps).

of *Volunteered Geographic Information* [12, 17]. Previous work on POI matching has shown that the median distance of a single POI between different geolocation service providers is 62.8 meters apart and can reach up to several hundreds meters under extreme circumstances (e.g., for a golf course) [18]. Figure 2 (left) illustrates this fact by showing the position of markers from five major services. While this offset may not be a substantial issue in rural areas due to their low POI density, it will cause substantial problems for geolocation services (e.g., check-in services) in high-density urban areas.

The task of determining the place an individual is visiting based on coordinates gathered from their mobile device becomes more difficult given the uncertainty associated with each POI in the dataset. That is, selecting the nearest POI to a user’s location becomes an artifact of the arbitrary point-coordinate representation of nearby POI. Leaving the actual POI locations aside, another facet of uncertainty plagues traditional geolocation services, namely the positional accuracy of a location-enabled device. While most devices make use of a range of positioning technologies (e.g., GNSS, WPS, Cellular Network), each of these technologies has its own issues related to accuracy, imparting a level of uncertainty on any device location. Therein lies one of the problems facing traditional geolocation services such as reverse geocoders. Given the aforementioned sources of uncertainty, how can a geolocation service be expected to accurately predict a POI from geographic coordinates? An example of this challenge is shown in Figure 2 (right). A number of POI are shown on the map along with their associated positional uncertainty. Additionally, the red pin shows the most probable location of a mobile device and its two-dimensional depiction of uncertainty.

## 2. Research Contribution and Example Scenario

Clearly, relying on geographic coordinates alone to infer a place based on a user’s mobile device position is not sufficient. However, there are other contextual clues that can be taken into account. Time is one such clue and in contrast to many other contextual information it is readily available with every position fix. Current reverse geocoding services solely exploit geographic location while in reality human behavior dictates that approximately the same location in geographic space can serve a variety of purposes at different times of the day or days of the week. The motivation for visiting a specific city block on a Tuesday morning is considerably different than visiting that same block on a Saturday night. While the geographic coordinates determined by one’s location-enabled mobile device may be temporally-agnostic, the *probability* of conducting an activity at a nearby place is not.

In fact, place categories are implicitly defined by time. For instance, the likelihood of being at the *Department of Motor Vehicles* on a Sunday at 1 AM is negligibly low. Not only is this likelihood driven



Figure 2: **Left:** Different services list different locations for *The French Press Café* in Santa Barbara, CA. Google Maps (G), OpenStreetMap (O), Foursquare (F), Yelp (Y), Bing Maps (B). **Right:** Uncertainty in POI location and user location. French Press Café (1) and Los Arroyos Mexican Restaurant (14). The red pin marks the user’s most probable location. Note that the circles of uncertainty are not drawn to scale; in actuality they would appear larger.

by socio-institutional constraints [23], but also by observable human-placial behavior patterns. Existing research in this area has shown that categories of places (e.g., Hospital, Restaurant, Bar) can be uniquely identified by the temporal patterns of their visitors [30, 19, 20]. In this work, we make the case for *time* being an additional readily available clue for reverse geocoding and geosocial check-ins in specific. We demonstrate that given a time-stamp of a location fix, *temporal signatures* [19] can be combined with existing distance-only methods to substantially enhance the accuracy of place estimations.

The research contributions of this work are as follows:

- In analogy to the notion of scale distortion in cartography, we present a model that uses temporal signatures to distort the location of POI relative to the query location and time, thereby reordering the set of potentially matching places. Using the check-in frequency of a POI category at a specific time, geographic space is distorted by a factor of the temporal probability. Places that show a high check-in frequency at the provided time are shifted closer to the queried geographic coordinates of the user while those with low probabilities are pushed further away. Intuitively, given a user’s location fix at 10pm, a nearby cinema is preferred over a closer bakery as the temporal signature of the place type *Bakery* indicates that people rarely visit bakeries during the night.
- We explore and report on multiple models for this temporal distortion analogy including linear, non-linear, symmetric and non-symmetric functions. Our study indicates that a non-linear, non-symmetric rational function produces the best results.
- We demonstrate the strengths of our method by evaluating it against a distance-only baseline (used by most currently available services) by determining the Mean Reciprocal Rank and the normalized Discounted Cumulative Gain.<sup>3</sup> Our enhanced method increases the estimated accuracy of an individual’s location Mean Reciprocal Rank from 0.359 to **0.453** and the normalized Discounted Cumulative Gain

<sup>3</sup>These statistical rank approaches will be further explained in Section 4.3.

from 0.583 to **0.711**. Additionally, we demonstrate that our model can also be used to improve the prediction accuracy of geosocial systems such as *Foursquare* which is noteworthy given their detailed ground-truth data.

- Several potential contextual clues are available to improve the quality of location services. Examples include weather information, mode of transportation, previously visited location, user preferences, and so forth. Many of these, however, are not available outside of commercial data silos, are difficult to mine, require different index schemes, or substantially increase the complexity of (pre-)computing candidate places. In contrast, time is readily available with every position fix and we provide signatures for over 400 place types for each hour of the week. Nonetheless, some use cases may require pre-computed results and cannot deal with this level of detail. By measuring information gain, we show that the temporal signatures vary greatly with respect to their indicativeness. Consequently, a few selected time-frames can already improve place estimation.
- Finally, we present an outlook on user-location distortion models. Our current work uses *default behavior* to compute the temporal probability of POI categories for different times. People (and places), however, do not always follow such established patterns. For instance, there might be an event at a location that would be closed otherwise. By enriching the default mode with a *dynamic real-time* model, we can adjust for such circumstances. We discuss the role of *Instagram* photos and *Tweets* to determine trending areas in real-time. We propose an inverse-distance weighed method to alter the user’s query location, pulling it closer to areas of high online-social networking popularity.

Stepping back from the research contributions for a moment, let us explore a real-world scenario depicting the problem. This scenario will act as running example throughout the paper. Figure 3 shows a query location (red pin) and a number of nearby POI. A standard distance-only approach would simply calculate the distance between each POI and the query location and return a ranked set of distances allowing the user to make the assumption that she is currently at the closest POI. In referencing the temporal signatures for the different POI types, we find a *visit probability value* for each category of POI at any given hour of the day on any day of the week.

Table 1 shows the categories associated with each POI in Figure 3, the geographic distance to the query location, as well as the temporal probabilities for those POI types at both 10 AM on Monday and 11 PM on Saturday. As one can see, the popularity of nearby POI change significantly between the two times. Rather than assuming that there is an equal likelihood of a user visiting a POI, irrespective of time and type, it follows that temporal probability should be included in determining the most likely visited place.

The remainder of the paper is structured as follows. In Section 3 we introduce the extracted temporal signatures, and the used data. Next, Section 4 discusses our temporal signatures-based location-distortion model, tested functions that realize these models, and their weights. In Section 5 we evaluate our proposed method. We present an outlook on dealing with real-time information in Section 6. In Section 7, we contrast our work to related research and discuss relevant findings. Finally, Section 8 offers conclusions and directions for future work.

### 3. Temporal Signatures and GeoSocial Check-in Data

In this Section, we introduce the temporal signatures and the data from which they were derived.

#### 3.1. Activity Categories

When a new POI is contributed through the Foursquare mobile application, the creator is able to assign a category tag by selecting from a pre-defined hierarchical set of activity categories. Originally generated by user-contributed tags, governors of the Foursquare application refined the list on multiple occasions, eventually restricting category assignments to just those provided via the application. While the set does occasionally undergo minor adjustments, at time of writing, this category set consists of 421 unique place types divided between three hierarchical levels [9]. Contributors to the application are asked to assign at

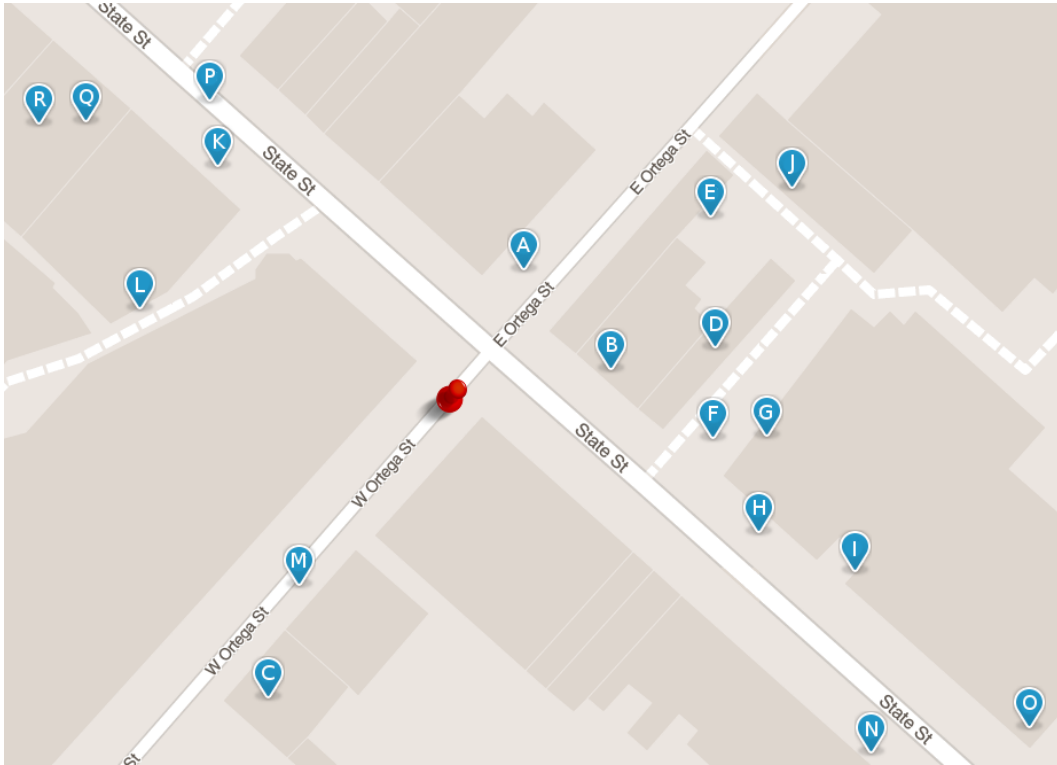


Figure 3: Coordinates from user’s device (red pin) and nearby POI (blue markers).

least one category to any venue they generate, though this is not enforced [10]. A sample<sup>4</sup> of 15,731,452 POI from across the United States showed that 86.19% of venues were assigned one categorical value, 13.74% had no category, and 0.07% had 2 or more categories.

### 3.2. Geosocial Check-ins

Geosocial *check-in* data were collected via the Foursquare API with the purpose of constructing temporal signatures for specific venue categories. A total of 908,031 randomly selected Foursquare venues<sup>5</sup> were accessed via the application API, divided amongst 421 categories, with a goal of accessing 240 venues per category. Unfortunately given the uniqueness of a number of categories (e.g., Molecular Gastronomy Restaurant) it was difficult to achieve this number of POI for each category. Once the venues were chosen, check-in data were accessed every hour for four months starting October 2013. Each request for check-in information returned a value of *HereNow* which indicates the total number of users checked-in to the specific venue at any given time. Provided the number of venues listed above, a total of 3,640,893 check-ins were temporally analyzed. To account for regional variations, the data was collected from Los Angeles, New York City, Chicago, and New Orleans.

It is worth noting that the Foursquare data is biased towards a particular user population, places, and place types. For instance, the typical Foursquare user is a 30-year-old American male and more likely to check-in at a trendy nightclub than a hospital. We mitigate this problem by aggregating the data to the type level, i.e., over millions of check-ins, even though some places and place types receive less check-ins, nightclub still peak during weekend nights, while airports have a more uniform high-entropy visiting probability throughout the day and week with dips in the late night/early morning. More importantly, however, our

<sup>4</sup>Accessed through the public-facing API

<sup>5</sup> *Venue* in this case is the Foursquare-specific term for Point of Interest

Marker	Category	Distance (m)	Monday 10AM $(10^{-3})$	Saturday 11PM $(10^{-3})$
A	Bakery	39.2	6.28	4.08
B	Nightclub	41.4	0.26	44.16
C	Nightclub	69.9	0.26	44.16
D	American Restaurant	62.7	1.61	9.50
E	Bakery	73.7	6.28	4.08
F	Fast Food	65.0	4.80	5.78
G	Apparel Store	85.8	2.51	1.09
H	Ice Cream Shop	82.6	0.84	15.88
I	Movie Theater	94.2	1.44	11.00
J	Pub	88.9	0.53	22.66
K	Cosmetics Shop	60.9	3.87	1.57
L	Diner	70.0	5.49	7.56
M	Italian Restaurant	45.7	1.42	7.96
N	Furniture / Home Store	114.9	4.79	5.01
O	Grocery Store	147.8	4.53	1.38
P	BBQ Joint	82.3	0.43	9.35
Q	Burrito Place	88.1	0.54	3.16
R	Italian Restaurant	93.6	1.42	7.96

Table 1: POI Categories shown on Figure 3 with distance to device location and temporal probabilities (sum of probabilities across all categories sums to 1) on Monday 10 AM and Saturday 11 PM.

work is concerned with studying the role of time for reverse geocoding and the different distortion models, not the particular geosocial dataset. Other data sources, e.g., from large-scale transportation surveys, could be used as well. Unfortunately, to the best of our knowledge, no alternative data sources with a similar spatial, temporal, and thematic resolution exist. Finally, the majority of geolocation services target a similar audience to Foursquare. We will revisit the Foursquare bias in the evaluation (Section 5).

### 3.3. Constructing Temporal Semantic Signatures

Provided *HereNow* values for every POI in the venue set, the values were aggregated by category, hour, and day of the week. The resulting 168 values for each category span every hour of a week. Normalizing this data by the total number of check-ins for each category shows the check-ins per hour as a percentage of the total week.

While these check-in data are limited to a four month time-span, the high resolution allows for temporal signatures to be constructed for each category. In visualizing the temporal distribution of the check-ins grouped by category, one can extract novel temporal patterns for each category in the set. These are called temporal *bands* and *signatures* in analogy to spectral signatures in remote sensing and follow a semantics-driven *social sensing* approach proposed in previous work [15, 1]. A semantic signature may be composed of one or multiple bands [1]. Simplifying, a signature is the minimal set of bands that jointly identify a place type. Figures 4 and 5 show daily and hourly temporal bands (respectively) for four POI categories that jointly form signatures to uniquely identify categories via the spatiotemporal behavior of users of location-based social networks.

Modeling the daily check-in bands separately from the hourly check-in bands exposes some interesting nuances in the data. Both *Wineries* and *Nightclubs* are social and entertainment venues that serve alcohol, and show very similar temporal check-in patterns over a week time period with peaks on the weekend. In contrast, the hourly temporal bands show a very different pattern. These data show Winery visits peaking in the mid-afternoon while nightclub check-ins peak late at night (very early morning). This presents an excellent example of why varying temporal scales are necessary for constructing robust temporal signatures. Figures 4 and 5 also depict a contrast between activities in which time plays a defining role, e.g., American

football games on Sunday afternoons, and those where temporal aspects are less indicative of a POI type, e.g., Airports.

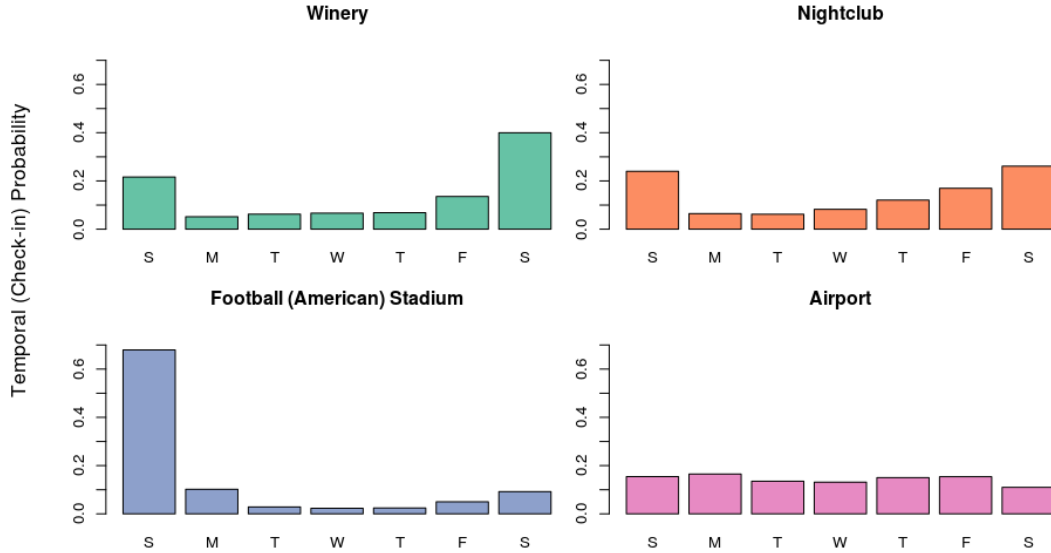


Figure 4: Daily temporal signatures for four POI categories.

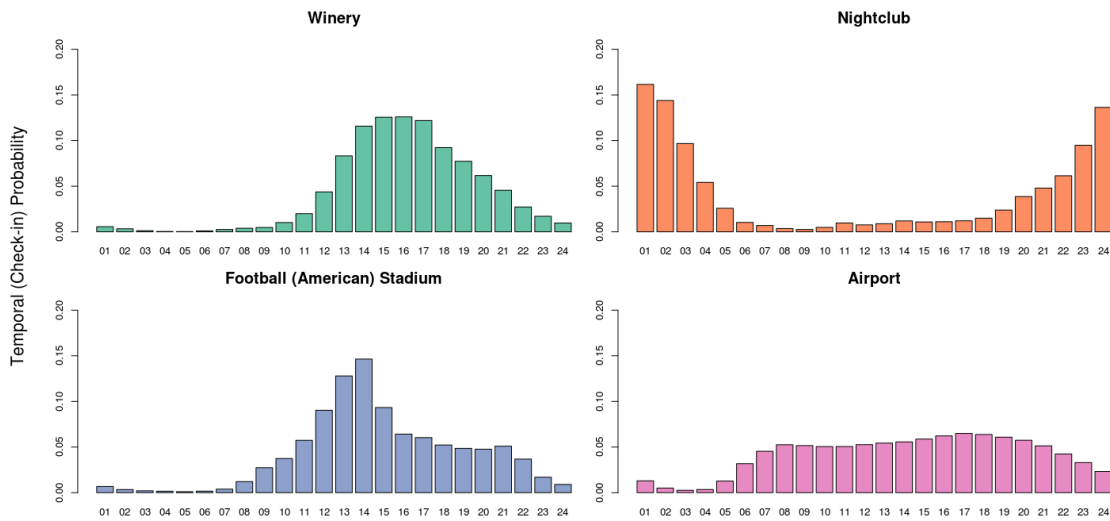


Figure 5: Hourly temporal signatures for four POI categories.

### 3.4. Indicativeness of Temporal Bands

This leads to the interesting question of which hours and days are most indicative and whether it is possible to compress the bands instead of storing all potentially relevant 168 values per POI type. To investigate this question, we look at the signatures from a classification perspective and consider each band as a discretized feature (attribute) of a class-labeled set of training tuples. Here, we use the entropy-based *information gain* as indicativeness measure. Equation 1 shows the computation of Shannon’s information

entropy for a distribution  $D$ , where  $p_i$  is the probability of band  $i$  and Equation 2 computes the information gain ( $\Delta(b_t)$ ) for a temporal band with  $\frac{|D_j|}{|D|}$  being the weight of the  $j$ th partition of the training set according to this band. Table 2 shows the 10 most indicative hours as well as the 10 least indicative hours. Intuitively, the typical lunchtime hours (11am-12pm), close of business hours (4-5pm), and dinner/nightlife hours (10-11pm) are most indicative of a POI type, as is the distinction between workdays and weekends. In contrast, the early morning hours, e.g., Monday 5am, are significantly less-indicative. Consequently, visiting probabilities at these times will not differ substantially between POI type and thus can be pruned without severely impacting the signatures to save storage or optimize indexing.

$$H(D) = - \sum_{i=1}^n p_i \log_2(p_i) \quad (1)$$

$$\Delta(b_t) = H(D) - \sum_{j=v}^n \frac{|D_j|}{|D|} \times H(D_j) \quad (2)$$

Band	Hour	Information Gain	Band	Hour	Information Gain
143	Friday 11pm	0.772	101	Thursday 3am	0.112
59	Monday 11am	0.750	150	Saturday 6 am	0.097
107	Thursday 11am	0.744	124	Friday 4am	0.093
60	Monday 12pm	0.725	26	Monday 2am	0.082
35	Sunday 11am	0.712	27	Monday 3am	0.079
161	Saturday 5pm	0.695	125	Friday 5am	0.063
88	Wednesday 4pm	0.693	28	Monday 4am	0.052
167	Saturday 11pm	0.69	100	Thursday 4am	0.046
142	Friday 10pm	0.688	149	Saturday 5am	0.045
131	Friday 11am	0.687	29	Monday 5am	0.034

Table 2: The 10 overall most indicative hours according to their information gain and the 10 least indicative hours.

#### 4. Temporal Signature-based Location-distortion

In this section we introduce the temporal signature-based location-distortion models and discuss concrete functions and their parametrization that realize these models.

##### 4.1. Distortion Models

The majority of current geolocation services take a position fix as input and return a list of ascending distance-ranked POI based on the geographic coordinates of those POI. Given a robust set of type-level temporal probabilities gathered from location-based social networking check-ins, this paper offers a model for increasing the accuracy of the distance-only approach through the inclusion of a temporal component. Different types of POI show fluctuations in visiting probabilities throughout the day. Based on check-in behavior, these fluctuations reflect increases and decreases in POI type popularity. We leverage these probabilities to enhance distance-only geolocation approaches. To do so, **we propose an analogy to scale distortion in cartography and distort space by a factor of the temporal probability**. That is, we pull or push POI in the users vicinity depending on their type’s visiting likelihood during a particular time of the day.<sup>6</sup> In the following, we discuss four possible models and potential functions for their realization (Figure 6) that alter the geographic distance between the query location and each POI by a weighted temporal probability.

<sup>6</sup>It is worth noting that all analogies are partial. We mathematically model the relative impact of distance and time to alter the POI ranking returned to the user but do not actually modify the underlying geo-data.

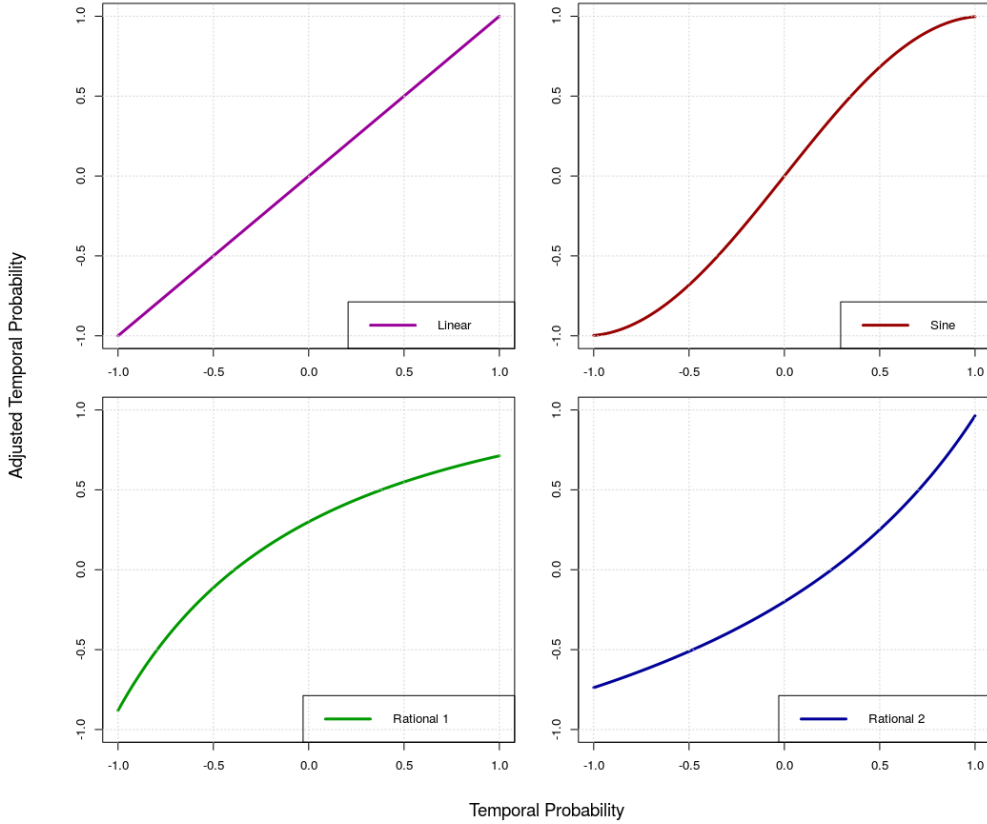


Figure 6: Four possible distortion models and examples of their realization for shifting POI locations based on the temporal probability of their types (e.g., restaurant); *exaggerated*.

These four models represent different approaches to combining distance and time. The *linear* approach *symmetrically* adjusts the distance by pushing POI with low check-in probabilities away from the query location at a linear rate equivalent to the amount that high-probability venues are pulled towards the query location. Alternatively, one could model a changing, i.e., *non-linear*, push/pull rate that changes with the probability. While still symmetrical in its design, the assumption underlying this model is that highly likely or unlikely places should be pulled or pushed at a different rate while values close to the mean should approximate a linear behavior. In Figure 6 (Sine), we employ a particular interval of a *sine* functions for the symmetric non-linear model. We also explore *non-linear, non-symmetrical* options. *Rational 1* shown in Figure 6 depicts an example of one such option. In this case, as the probability of a user checking in to a POI increases, the amount by which the distance decreases diminishes. Correspondingly, as the temporal probability decreases, the amount by which the distance increases grows. In other words, those POI with low check-in likelihoods are punished at a higher rate than those with high probabilities are rewarded. The inverse approach is also presented in Figure 6, *Rational 2*, decreasing the influence on geographic distance as temporal probability values move to the left while exponentially increasing the influence on distance as values move to the right. Intuitively, the rationale behind both non-linear, non-symmetrical models is to study whether pushing and pulling should be performed at different rates. Each of these four models is unique in its approach to the data and the distortion analogy. We compare them, their realizations by particular functions, and their parameterization next.

#### 4.2. Spatiotemporal Distortion Functions

To combine the temporal signatures with the existing spatial distance-based ranking, we introduce a new ranked-distance attribute,  $d_t$ , for each POI. The value of this attribute is defined as a distortion of

the existing geospatial distance (between the POI and the query coordinates) by a factor of the temporal probability. In determining the value of  $d_t$ , two steps must be taken: (1) We must select the function through which time and distance are combined. (2) The ratio of influence (weight) that both distance and time have on the new attribute must be determined.

Of the four approaches presented in Figure 6, the *linear* method was the first to be examined. To start, we calculated the mean of the temporal probability values,  $t'_m$ , for all venues nearby our query location. In order to determine if a given venue should be *pushed* or *pulled* from the query coordinates the temporal probability value of the given venue,  $t'$  is subtracted from this mean. The resulting variable,  $\tilde{t}'$ , indicates the direction (sign) and amount by which said venue's spatial distance ( $d_t$ ) should be distorted (Equation 3). Next, a weighted combination of the normalized distance and normalized temporal probability is calculated (Equation [linear-type](#)) where  $w$  is the assigned weight and  $d'$  is normalized spatial distance between the selected POI and the query coordinates. This approach adjusts the spatial coordinates of a chosen POI by increasing or decreasing the distance between the POI and the query coordinates linearly and symmetrically.

$$\tilde{t}' = t'_m - t' \quad \text{Where } t' \in [-1, 1] \quad (3)$$

$$d_t = d' \cdot w + \tilde{t}' \cdot (1 - w) \quad (\text{linear-type})$$

While effective, this *linear distortion* approach is restrictive. This method pushes and pulls all POI at the same rate, regardless of the amount by which their temporal probability value differs from the mean. An alternative approach is to use a non-linear function, e.g., a *sine* function. The *sine* function approximates the linear method as  $\tilde{t}'$  approaches zero, but decreases in magnitude of distortion as temporal probability values move away from zero. For this second approach,  $d_t$  as computed as shown in Equation [sine-type](#).

$$d_t = d' - \sin(\tilde{t}') \cdot w \quad (\text{sine-type})$$

Though appropriate for the data, the *sine* approach (for that particular interval) still assumes that POI on either side of the temporal mean should be distorted symmetrically. Thus, we explored non-symmetric models with the purpose of decreasing the distortion of the temporal probability on the positive side of the mean at a greater rate than those values on the negative side of the mean (for instance). We modeled this by employing a weight-adjusted rational function (Equation [rational-type 1](#)). The inverse approach was also modeled as shown in Equation [rational-type 2](#). Relaxing the symmetry requirement makes the statement that those POI that are less probable (of being visited at the given time of the day/week) should arguably be pushed further away from the query location at a higher rate than those being pulled closer.

$$d_t = d' - \left(1 - \frac{w}{\tilde{t}' + w}\right) \quad (\text{rational-type 1})$$

$$d_t = d' - \left(\frac{w}{-\tilde{t}' + w} - 1\right) \quad (\text{rational-type 2})$$

Each of the methods discussed in this section offers a unique perspective on the *push / pull* approach to spatial distance distortion. While countless other methods could potentially be evaluated, these four approaches cover the fundamental concepts necessary for this work, namely, *symmetric vs. non symmetric* and *linear vs. non linear* distance distortion.

### 4.3. Weights

In the next step we determined the most suitable weight ratio between the normalized distance and the normalized temporal probabilities by using a set of geosocial check-in test data.

Using the *Twitter Streaming API* [27], 3,500 geolocated *Foursquare check-ins* were sampled from within the Greater Los Angeles region between November 1st and November 20th, 2013. The geographic coordinates as well as the category of the POI in which the Twitter user checked in were accessed. The number of check-ins (and the associated POI) were reduced to 2,800 to ensure that only those POI that showed at least 15

other POI within a 100 meter radius were included in the sample. This restriction ensured that the results were not biased due to a lack of available POI from which the model could make a selection.

The geographic coordinates of these 2,800 check-ins/POI were employed as the base *user* locations from which the geolocation model would be built. In order to mimic the accuracy of a GPS enabled mobile device and arbitrariness in point-feature placement, a location-uncertainty component was introduced. Altered test locations were drawn from a normal distribution with a mean of 30 meters and standard deviation of 10 meters from the POI’s known geographic location (from Foursquare). The directional (angular) offset was randomly assigned for each set of coordinates. These coordinate values were taken as individual *user locations* which then formed the basis on which the geolocation model could be trained. As discussed in the introduction section this is a very conservative estimate of the involved positional uncertainties. Stronger shifts in position would additionally favor our time-enabled method.

Provided these test user locations, a baseline test was developed. Each of the 2,800 test locations were queried against a comprehensive set of 15,729 POI and all POI within a 100 meter radius of each queried test user location were returned and ranked by geographic distance from shortest to longest. The ranked position of the POI known to be the user’s true check-in location was recorded for each scenario and the *Mean Reciprocal Rank (MRR)* was then calculated for the overall test results. MRR, shown in Equation 4, is a statistical measure for evaluating the results of a ranked set of  $N$  (Number of POI in this case) responses.

$$MRR = \frac{1}{|N|} \sum_{i=1}^{|N|} \frac{1}{rank_i} \quad (4)$$

Using the *distance-only* MRR as a baseline, we tested which combination of weight and function maximized the MRR value, i.e., we quantified the relative importance of time for reverse geocoding as well as the particular distortion model that would yield the best results. Four other sets of MRR values were calculated based on the combination of temporal probability with geographic distance using each of the four functions discussed earlier (Figure 6). Each model was tested multiple times with a weight value increasing from zero at increments of 0.1. Figure 7 shows that all of the weighted functions out-perform the distance-only method at some point.

To validate this finding and ensure that the selected functions and weights are not merely an artifact of using MRR as the measure, we computed additional rank comparison measures. A sum of the reciprocal rank (SRR) method was explored as well as counting the number of correctly identified POI (rank position 1). Finally, the popular normalized Discounted Cumulative Gain (Equation 5) measure was computed for each of the functions where *DCG* is defined by Equation 6 and *POIcount* is the number of POI identified at the specified  $i$ th ranked position. *IDCG* is the *ideal* discounted cumulative gain which in this case is 2,800 given that an ideal result would correctly identify all POI in the first ranked position. The maximum MMR values, SSR, nDCG and first ranked position count along with their associated weights for each function are shown in Table 3 indicating that the Rational 1 based model produces the best overall results with a weight of 2.8. It is worth noting that the linear model only performs well within a narrow band of weight values and that the Rational 1 approach continues to perform well with high weight values.

$$nDCG = \frac{DCG}{IDCG} \quad (5)$$

$$DCG = POIcount_1 + \sum_{i=2}^N \frac{POIcount_i}{\log_2(i)} \quad (6)$$

Taking this result, we revisited our running example introduced in Section 2 and distorted the query location and the POI locations by shifting them closer or further away. Figure 8 depicts this adjustment given a query time of 10 AM on Monday morning. The original distance from the query location to each POI is shown in the table and the original locations are shown as faded markers on the map. The new distorted distances are listed in the table as well as shown on the map via the bright blue markers. By comparison, Figure 9 shows the same process for 11 PM on Saturday night. Note that in the original distance-only

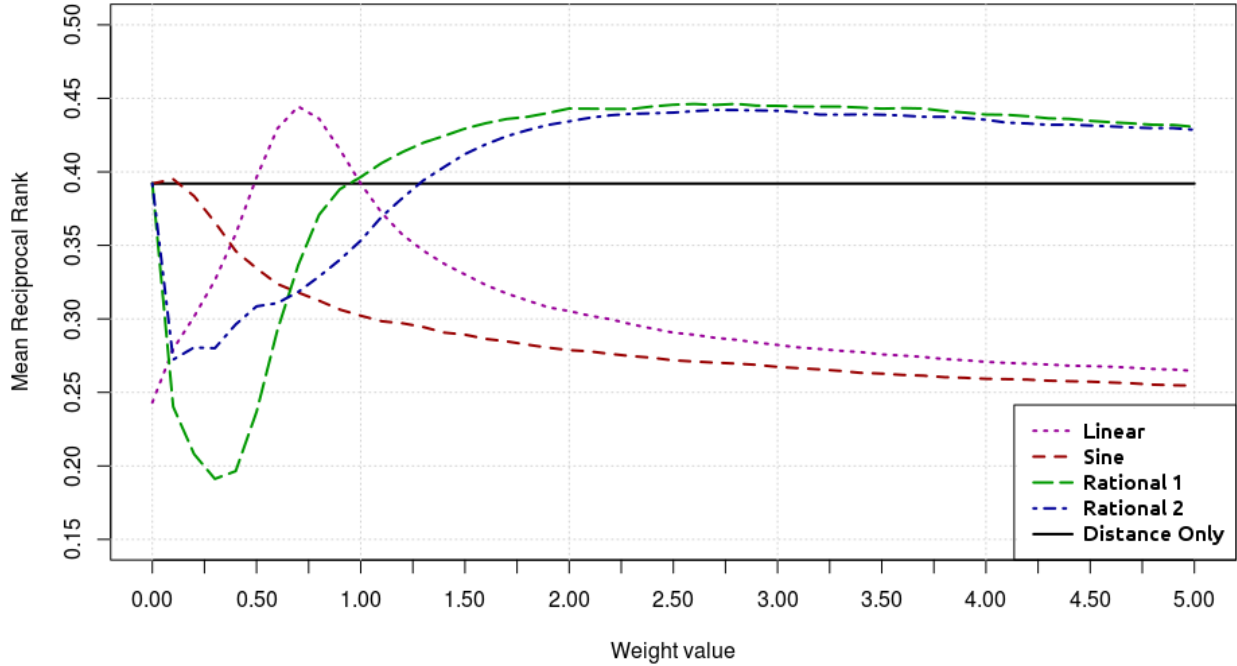


Figure 7: Mean Reciprocal Rank for Four Equation and associated weight values compared to Distance-only.

Function	Max MRR	Max SRR	nDCG	First Pos.	Weight
Distance Only	0.392	1095	0.621	485	NA
Linear	0.444	1245	0.665	661	0.7
Sine	0.395	1154	0.642	539	0.1
<b>Rational 1</b>	<b>0.446</b>	<b>1250</b>	<b>0.669</b>	<b>665</b>	<b>2.8</b>
Rational 2	0.442	1239	0.662	657	2.7

Table 3: Maximum Mean Reciprocal Rank (MRR), Maximum Sum of the Reciprocal Rank (Max SRR), normalized Discounted Cumulative Gain (nDCG), Number of POI ranked in the first position and associated weight for each Equation.

scenario (see Figure 3), the distance to the Bakery (A), the Nightclub (B), and the Italian Restaurant (M) are similar where the distorted cases lists very different distances with the Bakery (A) being nearest in Figure 8 and the Nightclub (B) being closest in Figure 9. The marker colors of these POI switch from red to green and vice versa between the two figures indicating a pull (green) or push (red) from the query location. Additionally, note that the Italian Restaurant (M) remains red between both figures indicating that it is not a very probable location at either time.<sup>7</sup>

## 5. Evaluation and Discussion

In order to test the validity of the temporally weighted geolocation approach, we designed an experiment with geosocial user data that tests the selected non-linear non-symmetric model with a weight of 2.8 against a distance-only based approach for a new test set of known locations and check-ins.

Specifying the Greater Los Angeles region as the boundary, the *Twitter Streaming API* was used to collect tweets that shared a Foursquare check-in. When a user of the Foursquare application decides to

<sup>7</sup>Keeping in mind that those temporal signatures are derived from data from the US and certain POI type are expected to have varying signatures across cultures, countries, and regions.

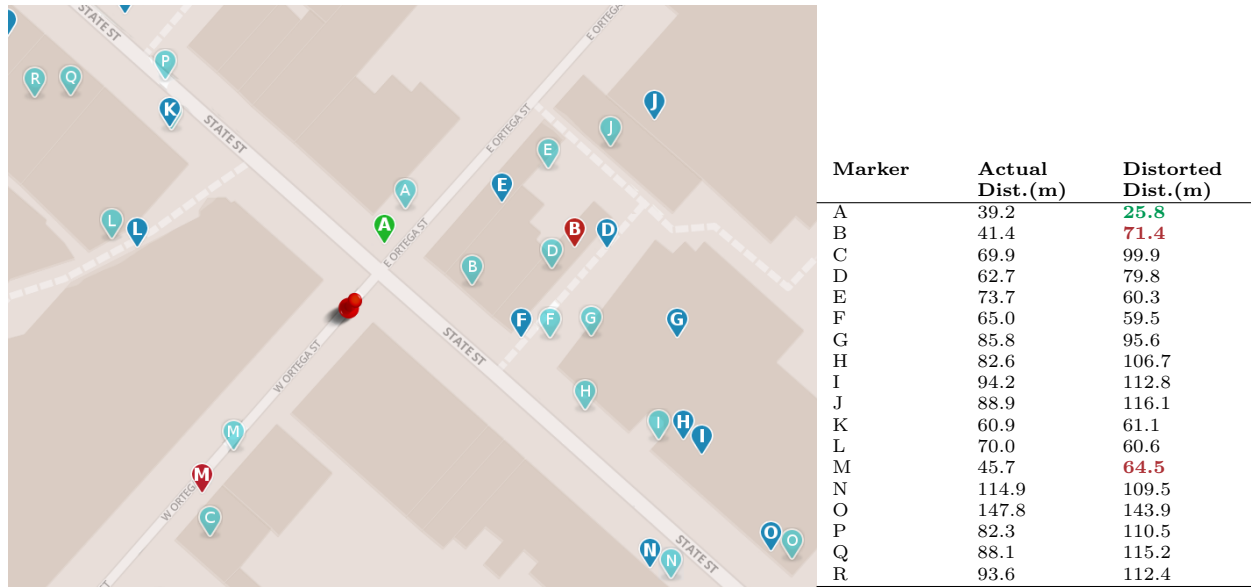


Figure 8: Nearby POI locations (dark blue markers) adjusted by temporal probability at 10AM on Monday. Original POI locations visible as light blue markers. Three example locations (A, B, M) are shown in red, indicating pushed further away and green, indicating pulled closer to the assumed user location.

check-in to a place, they are given the option of sharing this data on their Twitter Feed. While Foursquare check-in data itself is not publicly available, the majority of Twitter feeds are. Using this method, 1,663 unique check-ins were accessed over a 24 hour period.

Immediately on receipt of the check-in data, the geographic coordinates of the POI were randomized using the method described in Section 4.3 to reflect standard GPS inaccuracy and a new set of geographic coordinates were established for the user. These *user* coordinates were queried against the Foursquare Venues API (with the *Intent* parameter set to *Browse*<sup>8</sup>) and a set of 30 nearby POI were returned containing the distance from the query coordinates, *HereNow* (number of Foursquare users currently checked in to the POI), and *TotalCheckins* (total number of all-time check-ins to a specific POI).

Additionally, a separate query was made to the Foursquare Venues API with the *Intent* parameter set to *Checkin*. According to the Foursquare documentation *Browse* takes a distance-only approach to querying the gazetteer returning a set of nearby POI ordered by distance from query location, shortest to longest. Thus, the *Browse* mode is equivalent to most available geolocation services. The *Checkin* approach is not fully explained in the documentation and simply states that the returned set of POI are ordered based on where a typical user is likely to check-in to at the provided latitude and longitude at the current moment in time. This option is most likely based on the company’s internal popularity counts. In addition to the *Intent* parameter, each query was executed with additional parameters that specified a radius of 100 meters and minimum of 20 and maximum of 30 nearby POI. This limited bias due to a lack of nearby places.

Provided the set of nearby POI returned for each of the 1,663 queried *user* locations, the *distance-only* method can be compared against our new *temporal signatures* enhanced method. Since the actual POI to which the user checked in is known, it is possible to calculate a number of different measures for each approach. Table 4 presents the difference between these two methods across MRR, SRR, nDCG and 1st positions measures. The table shows that the inclusion of the temporal signatures model with a weight of 2.8, substantially outperforms the *distance only* method over all measures. In fact, the mean reciprocal rank (MRR) values rise from 0.359 to 0.453, an increase of **26.34%** and the nDCG values increase by **21.96%**.

Ranking the POI based purely on *TotalCheckins* produces a MRR of 0.678. Such a large discrepancy in numbers between *distance-only* and *TotalCheckins* method is an important reminder of how biased the

<sup>8</sup>Foursquare offers four methods for querying their gazetteer: browse, checkin, global and match.

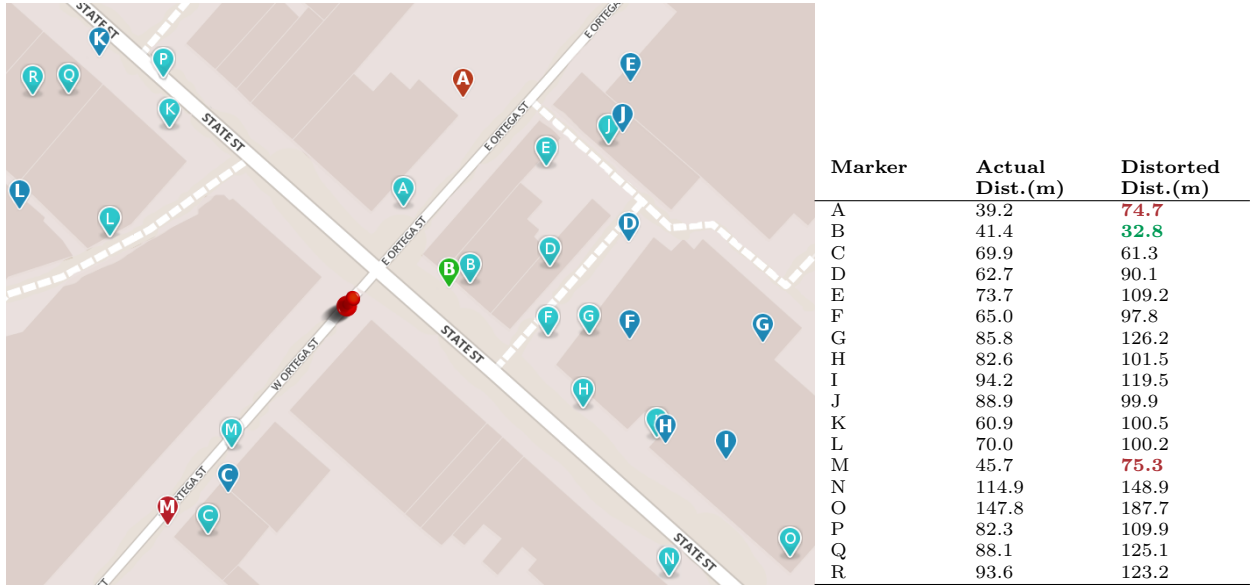


Figure 9: Nearby POI locations adjusted by temporal probability at 11PM on Saturday. Original POI locations visible as light blue markers. Three example locations (A, B, M) are shown in red, indicating pushed further away and green, indicating pulled closer to the assumed user location.

Method	MRR	SRR	nDCG	1st Pos.
Distance-Only	0.359	443.8	0.583	211
Temporally Adjusted	0.453	793.5	0.711	423

Table 4: Comparing the results of the Distance Only method to our method which includes temporal signatures.

Foursquare data and its users are, i.e., a very high percentage of the total user base predictably visits a small number of establishments. While *TotalCheckins* works well for an application such as Foursquare, the majority of geolocation services do not rely on a closed community and explicit check-ins from their users, but have to estimate the place based on space (and time) alone. Interestingly, adding our temporal distortion method to *TotalCheckins* can further improve Foursquare’s results. If we use the *TotalCheckins* values in lieu of geographic distance, first normalizing the values and then subtracting them from 1. This resulted in an MRR value of 0.692 a **2.1%** increase over *TotalCheckins* alone.

The *HereNow* approach (ranking POI by the number of users currently checked in) to determining a user’s placial location is self fulfilling. Note that this validation model is based on real check-in data and ranking a set of nearby POI based on the number of users currently checked in will always involve a high degree of bias. The correct POI will always have at least one current check-in. Examining Table 5, the influence of this bias becomes immediately apparent. The vast majority of POI do not show a single current check-in with a limited few listing 1. Were this example scenario to be run multiple times, one would expect the known POI to be correctly identified half of the time and the POI ranked 6th in the list (also showing a *HereNow* value of 1) to be identified half of the time. This *tie*, so to speak, can be broken through the inclusion of temporal signatures. Again, replacing the  $d'$  variable with the normalized *HereNow* value subtracted from 1, Equation [rational-type 1](#) is applied resulting in a **3.1%** increase and MRR measure of 0.872.

Lastly, Foursquare’s closed check-in method is examined. It must be reiterated that while the Foursquare method does produce a very high MRR value (0.733) it relies on data not available to most geolocation services and involves a significant amount of user bias which is likely exploited by this method [25]. Though its performance is strong, it may be further enhanced through our temporally-enhanced method. In this

POI ID	Distance(m)	TotalCheckins	HereNow
<b>4bba348c53649c746bc248fb</b>	<b>16</b>	<b>1398</b>	<b>1</b>
4d14fbb981cea35d9e80d7ec	16	705	0
4a52bc1cf964a520f7b11fe3	22	479	0
4af22b13f964a5204be621e3	24	877	0
4acbf6abf964a52077c820e3	29	900	0
51301edfe4b01507da6114f2	37	675	1
516327d7e4b063c6e8320956	41	8	0
4a12b3baf964a5208e771fe3	43	3282	0
4e01174b1f6ef39c29422260	45	2560	0
4cd19cf9f6378cfa8e8abcd6	45	59	0

Table 5: Example of Foursquare Search API query results ordered by distance and limited to 10. Known check-in location in bold face.

case, the nearby POI returned from the search query are assigned a rank value based on their order within the set. This ranked value is normalized and assigned to the  $d'$  variable in the [rational-type 1](#) equation. The resulting MRR of 0.747 is **2%** higher than the proprietary-only approach showing that even a calibrated, in-house built method can be improved upon through the inclusion of temporal signatures.

## 6. The Next Step: Geosocially Distorting the User’s location

The previous sections discussed a novel method for distorting the geographic location of POI based on the temporal probability of an individual visiting these POI as determined by their type. Additionally, in this section we outline a model that focuses on distorting the geographic location of the *user’s device location* based on the presence of geosocial activity nearby. The geosocial activity referred to in this case pertains to trending online activities such as *geotagged tweets* and *geotagged Instagram photographs* that do not include placial tags but are tagged with geographic coordinates. Since these posts cannot be directly assigned to POI, they cannot influence the amount and direction by which a POI location is distorted. Instead, these activities impact the ability to geolocate an individual through distorting the actual query coordinates themselves.

Figure 10 presents an example scenario. The blue markers on the map indicate the location of POI, similar to figures shown previously. Instagram (camera icon) and Twitter ( $t$  icon) markers are shown on the map as well. These geosocial activities are collected over a one hour time period. In looking at this map, it is apparent that an event is occurring at the plaza (green region) given the high number of tweet and photo activity in the past hour. Combining this information with the knowledge that the user’s query location is subject to uncertainty, adjusting the query location closer to the plaza is a reasonable proposal.

Using vector addition, a new vector is calculated from which distortion direction is ascertained. The *amount* by which the query location is adjusted is based on two factors. An inverse distance weight is calculated for each geosocial activity, assigning a greater weight to nearby activities than those occurring further away. Note that actual content of the tweet or Instagram caption is irrelevant in this approach. While some individual’s may prefer one source of social content over another, for our purposes, all geosocial activities are of equal value, their influence on the query coordinates are based solely on distance and direction. The second factor influencing the distortion is the global weight value with which the combination of these activities influence the query location. This global weight is the focus of future research and will involve additional training in order to establish an optimal value.

It is worth noting that we do not assume that the presence of a Tweet or Instagram photo in a specific region indicate that this is the only area where an activity is occurring. This approach takes the presence of geosocial data as an additional and readily viable variable that can be employed to better geolocate an individual based on locations that are currently *trending*. This method makes the assumption that the presence of a tweet or photo represents an increase in probability that some activity is taking place at this location.

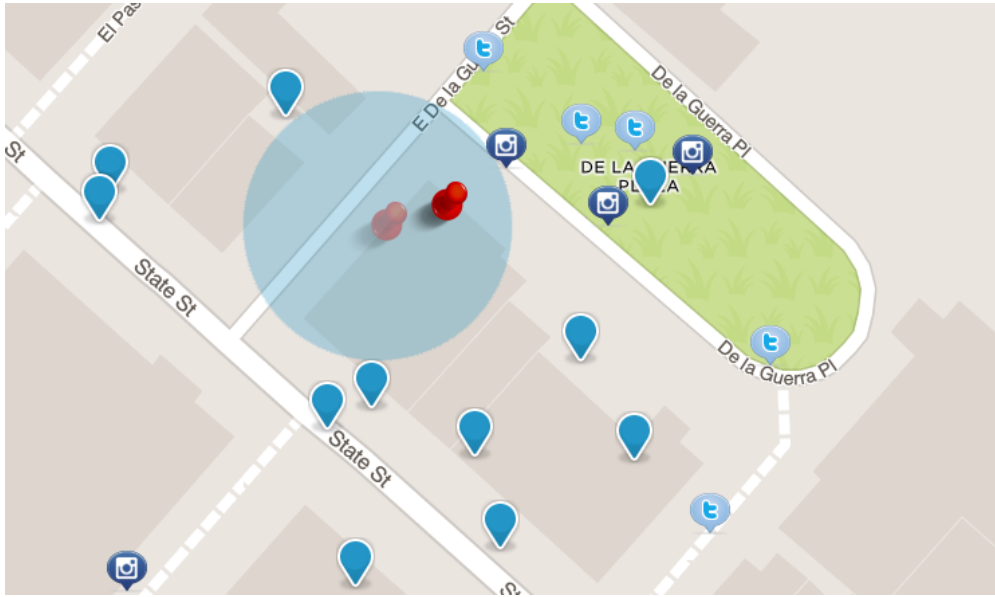


Figure 10: Example visualization of a user’s actual location (faded red pin), adjusted location (bright red pin), location uncertainty (large blue circle), Foursquare POI (blue markers) and Twitter and Instagram activity markers.

Intuitively, the temporal signatures-based method introduced in this paper exploits assumptions about the *default* behavior of people, e.g., nightclubs are visited predominantly on weekend nights. In contrast, adjusting the user’s potential location towards centers of (real-time) activity as observed from social media gives us the possibility to deviate from the default behavior. We call this the *bust-mode* to indicate that it overrides the default view on place and time [19]. The difference between default and burst mode could also be applied for other tasks in the future, e.g., for anomaly detection.

## 7. Related Work

Existing research on user and mobile device specific geolocation services can be split in to two roughly defined groups. One approach focuses on the technical aspects associated with determining one’s location, increasing the accuracy of location-based technologies [26, 7] as well as enhancing the efficiency of location services on mobile devices [24, 21]. For better or worse, these advances are reflected in a number of patents filed recently [33, 4]. While useful, these approaches do not consider non-technical sources of geolocation information, but instead focus on reducing the uncertainty associated with a device’s geographic coordinates.

The second approach has arisen from place recommendation research. Many of these approaches take advantage of the rise in geosocial check-ins and posts to explore user-similarity, [16, 5, 29] as well as user’s home locations [2, 14]. Additionally, recent work has begun to explore temporal patterns in user behavior through online social networking check-ins [11, 6] as well as human mobility patterns through mobile device tracking [32, 22]. Shaw et al. [25] explored the use of check-in data for enhancing venue search results in the Foursquare application. While the authors did investigate both the temporal and spatial components of check-ins, they did so without exploiting category types. Additionally, their methodology for merging spatial and temporal data is sparse and clearly does not consider distorting space by a function of time. Lastly, though their work does produce promising results, these results are specific to the Foursquare application and founded on a level of data-access restricted to Foursquare employees and thus of limited use to the reverse geocoding community outside of the company.

From a temporal signatures perspective, early work by Ye et al., [30] extracted check-in behavior from the online location-based social network *Whrrl* to determine daily and hourly default temporal patterns for a number of Whrrl place types. Yuan et al. [31] took this a step further using these temporal patterns to

recommend points of interest based on the time of day. Furthermore, Wu et al. [28] show how social media check-in data can be used for combining a movement-based approach with activity-based analysis in studying human mobility patterns. In exploring Flickr data, Hauff [13] recently found that the popularity of venues plays an important role (orders of magnitude) in the accuracy of geotagged Flickr photos. Additionally, a large study on mobile phone usage by Yuan et al. [32] found unique activity patterns based on age and gender indicating that temporal signatures may differ not only by POI category, but also by visitor demographics.

While much of this work has focused on extracting user behavior from social-sharing platforms, it has been used to estimate, predict or make recommendations on places an individual may have visited (past) or should/may visit (future). To the authors' knowledge, very little research has focused on using existing public, place-based check-in behavior to enhance existing technical approaches to geolocation in real-time. Additionally, no published work can be found that distorts geographic distance by a factor of temporal probability.

## 8. Conclusions & Future Work

The striking increase in location-based mobile applications in recent years is driving the need for better and more accurate geolocation services to the forefront of geo-computational research. Compounded by the inaccuracies of user-generated geo-content, positioning technologies, arbitrariness of the point-feature based representation of places, and to forth, the need for geolocation methods built on more than mere Euclidean distance are a necessity. Online geosocial networking solutions now offer researchers the ability to study human activity behavior which supply the foundation for categorically unique check-in signatures. By incorporating these semantic signatures with existing distance-only based geolocation services, more accurate results can be ascertained.

In this paper we demonstrate a novel technique for incorporating temporal signatures with geographic distance by virtually distorting (pushing and pulling) the geographic coordinates of nearby Places of Interest. In order to achieve the highest accuracy, a non-linear, non-symmetric approach was employed significantly outperforming the distance-only based geolocation service. Additionally, this same method was used to enhance existing state-of-the-art check-in and proprietary methods offered by top mobile applications on the market today. Finally, we outline a method for the enhancement of this approach through the use of geotagged social content such as *tweets* and *Instagram photographs*.

Future work in this area will include the continued enhancement and fine-tuning of the existing temporal signature weight and function. The methods above outline one possible technique for incorporating time with spatial reverse geocoding and future work will focus on improving the formula as well as including geosocial activities outlined in Section 6. While the method used in this work improved upon the distance-only baseline by between 12-26% for MRR (and has high as 50% for *1st Position Ranking*), another sample set from another region may produce slightly different results. A limitation of this work is evident in the three month span of data collection. An increase in the temporal extent of the data will allow further research into seasonal effects, holidays and climate fluctuation to name a few. Additional work aims to investigate regional variance in categorical-temporal signatures (e.g., Nightclubs in New York vs. Nightclubs in Los Angeles) as well as the influence of local weather patterns and daylight effects. The enhancement of the existing dataset will serve to increase the accuracy and robustness of the temporal signatures-based approach. Finally, an online service is in development that will allow interested parties to increase the accuracy of existing services in real-time and over large datasets.

## References

- [1] Adams, B., Janowicz, K., 2015. Thematic signatures for cleansing and enriching place-related linked data. *International Journal of Geographical Information Science* (ahead-of-print), 1–24.
- [2] Backstrom, L., Sun, E., Marlow, C., 2010. Find me if you can: improving geographical prediction with social and spatial proximity. In: *Proceedings of the 19th international conference on World wide web*. ACM, pp. 61–70.
- [3] Bowling, E., Shortridge, A., 2010. A dynamic web-based data model for representing geographic points with uncertain locations. In: *Spatial Accuracy Symposium 2010*. pp. 1–4.

- [4] Brewington, B. E., Brown, B. G., Guggemos, J. A., Hawkins, D., Stout, B., Sep. 10 2013. Augmentation of place ranking using 3d model activity in an area. US Patent 8,533,187.
- [5] Cheng, H., Arefin, M. S., Chen, Z., Morimoto, Y., 2013. Place recommendation based on users check-in history for location-based services. *International Journal of Networking and Computing* 3 (2), 228–243.
- [6] Cheng, Z., Caverlee, J., Lee, K., Sui, D. Z., 2011. Exploring millions of footprints in location sharing services. *ICWSM 2011*, 81–88.
- [7] Fallah, N., Apostolopoulos, I., Bekris, K., Folmer, E., 2013. Indoor human navigation systems: A survey. *Interacting with Computers* 25 (1), 21–33.
- [8] Flickr, 2014. Flickr developer documentation.  
URL <http://www.flickr.com/services/api/flickr.places.findByLatLon.htm>
- [9] Foursquare, 2014. Foursquare category hierarchy.  
URL <https://developer.foursquare.com/categorytree>
- [10] Foursquare, 2014. What is the style guide for adding and editing places?  
URL <http://support.foursquare.com/hc/en-us/articles/201064960-What-is-the-style-guide-for-adding-and-editing-places>
- [11] Gao, H., Tang, J., Hu, X., Liu, H., 2013. Exploring temporal effects for location recommendation on location-based social networks. In: *Proceedings of the 7th ACM conference on Recommender systems*. ACM, pp. 93–100.
- [12] Harvey, F., 2014. We know where you are. and were more and more sure what that means. In: *Emerging Pervasive Information and Communication Technologies (PICT)*. Springer, pp. 71–87.
- [13] Hauff, C., 2013. A study on the accuracy of Flickr’s geotag data. In: *Proceedings of the 36th international ACM SIGIR conference on Research and development in information retrieval*. ACM, pp. 1037–1040.
- [14] Hecht, B., Hong, L., Suh, B., Chi, E. H., 2011. Tweets from Justin Bieber’s heart: the dynamics of the location field in user profiles. In: *Proceedings of the SIGCHI Conference on Human Factors in Computing Systems*. ACM, pp. 237–246.
- [15] Janowicz, K., 2012. Observation-driven geo-ontology engineering. *Transactions in GIS* 16 (3), 351–374.
- [16] McKenzie, G., Adams, B., Janowicz, K., 2013. A thematic approach to user similarity built on geosocial check-ins. In: *Geographic Information Science at the Heart of Europe, Proceedings of the 2013 Association of Geographic Information Laboratories in Europe Conference (AGILE ’13)*. Springer, pp. 39–53.
- [17] McKenzie, G., Janowicz, K., 2014. Coerced geographic information: The not-so-voluntary side of user-generated geo-content. In: *Extended Abstracts of the Eighth International Conference on Geographic Information Science*.
- [18] McKenzie, G., Janowicz, K., Adams, B., 2014. A weighted multi-attribute method for matching user-generated points of interest. *Cartography and Geographic Information Science* 41 (2), 125–137.
- [19] McKenzie, G., Janowicz, K., Gao, S., Yang, J.-A., Hu, Y., In Press. POI Pulse: A multi-granular, semantic signatures-based approach for the interactive visualization of big geosocial data. *Cartographica: The International Journal for Geographic Information and Geovisualization*.
- [20] Noulas, A., Scellato, S., Mascolo, C., Pontil, M., 2011. An empirical study of geographic user activity patterns in foursquare. *ICWSM 11*, 70–573.
- [21] Paek, J., Kim, J., Govindan, R., 2010. Energy-efficient rate-adaptive GPS-based positioning for smartphones. In: *Proceedings of the 8th international conference on Mobile systems, applications, and services*. ACM, pp. 299–314.
- [22] Palmer, J. R., Espenshade, T. J., Bartumeus, F., Chung, C. Y., Ozgencil, N. E., Li, K., 2013. New approaches to human mobility: Using mobile phones for demographic research. *Demography* 50 (3), 1105–1128.
- [23] Raubal, M., Miller, H. J., Bridwell, S., 2004. User-centered time geography for location-based services. *Geografiska Annaler: Series B, Human Geography* 86 (4), 245–265.
- [24] Schilit, B. N., LaMarca, A., Borriello, G., Griswold, W. G., McDonald, D., Lazowska, E., Balachandran, A., Hong, J., Iverson, V., 2003. Challenge: Ubiquitous location-aware computing and the place lab initiative. In: *Proceedings of the 1st ACM international workshop on Wireless mobile applications and services on WLAN hotspots*. ACM, pp. 29–35.
- [25] Shaw, B., Shea, J., Sinha, S., Hogue, A., 2013. Learning to rank for spatiotemporal search. In: *Proceedings of the sixth ACM international conference on Web search and data mining*. ACM, pp. 717–726.
- [26] Tawk, Y., Tomé, P., Botteron, C., Stebler, Y., Farine, P.-A., 2014. Implementation and performance of a GPS/INS tightly coupled assisted pll architecture using mems inertial sensors. *Sensors* 14 (2), 3768–3796.
- [27] Twitter, 2014. Twitter developer documentation.  
URL <https://dev.twitter.com>
- [28] Wu, L., Zhi, Y., Sui, Z., Liu, Y., 2014. Intra-urban human mobility and activity transition: Evidence from social media check-in data. *PloS one* 9 (5), e97010.
- [29] Xiao, X., Zheng, Y., Luo, Q., Xie, X., 2010. Finding similar users using category-based location history. In: *Proceedings of the 18th SIGSPATIAL International Conference on Advances in Geographic Information Systems*. ACM, pp. 442–445.
- [30] Ye, M., Janowicz, K., Mülligann, C., Lee, W.-C., 2011. What you are is when you are: the temporal dimension of feature types in location-based social networks. In: *Proceedings of the 19th ACM SIGSPATIAL International Conference on Advances in Geographic Information Systems*. ACM, pp. 102–111.
- [31] Yuan, Q., Cong, G., Ma, Z., Sun, A., Thalmann, N. M., 2013. Time-aware point-of-interest recommendation. In: *Proceedings of the 36th international ACM SIGIR conference on Research and development in information retrieval*. ACM, pp. 363–372.
- [32] Yuan, Y., Raubal, M., Liu, Y., 2012. Correlating mobile phone usage and travel behavior—a case study of harbin, china. *Computers, Environment and Urban Systems* 36 (2), 118–130.
- [33] Zeto III, M. J., Rippetoe, D., Shaw, D., Mercer, A. R., Gaxiola Jr, G., Williams, R. T., Johansson, E. A. O., Jun. 6 2013. System and methods for delivering targeted marketing content to mobile device users based on geolocation. US Patent App. 13/911,956.